Bismuth Electrochromic Device with High Paper-Like Quality and High Performances

Michiya Nakashima,*,† Toshihiro Ebine,† Masami Shishikura,† Katsuyoshi Hoshino,*,‡ Kazunari Kawai,† and Kazuaki Hatsusaka†

Central Research Laboratories, DIC Corporation, 631 Sakato, Sakura, Chiba 285-8668, Japan, and Graduate School of Advanced Integrated Science, Chiba University, 1-33 Yayoi-cho, Inage-ku, Chiba 263-8522, Japan

ABSTRACT An electrochromic-type electronic paper was prepared using nanocomposites that consisted of silica nanoparticles (silica 60 wt %) and polyamide pulp. Its light scattering, ion transport, and aqueous electrolyte retention characteristics were examined. As a result, the shape of the nanocomposites was completely self-standing, though it could be impregnated with about nine times as much water on a weight basis. Moreover, its light scattering property was extremely similar to paper. Because of the impregnation of a large amount of water, the ion transport property of the nanocomposites was the same as that of the electrolyte solution without the nanocomposites. The nanocomposites was impregnated using an aqueous solution in which bismuthyl perchlorate (redox species), copper perchlorate, perchloric acid, sodium perchlorate, hydroquinone (electron mediator) and 2-buthyne-1,4-diol (leveling agent) were dissolved. The electronic paper was then prepared by sandwiching the nanocomposites between an indium−tin-oxide transparent electrode and a copper sheet. This electronic paper utilizes the reversible codeposition reaction of black Bi−Cu from bismuthyl perchlorate and copper(II) ions. The characteristics of this electronic paper were examined, and excellent characteristics with a white reflectivity of 65%, black reflectivity of 6.4%, contrast ratio of 10:1, operating life of over 1×10^6 cycles and open-circuit memory of at least 1 month were obtained. In addition, its driving voltage was 1.2 V, and the write time was 500 ms.

KEYWORDS: polyamide • silica • nanocomposites • electronic paper • bismuthyl perchlorate

1. INTRODUCTION

Electronic paper (reflective type display) (1−7) is expected to be a new display device that has the functions of both a display to which images are freely rewritten and paper, which is easy to read and quite portable. To satisfy the requirement that the image can be easily observed and eyes do not tire regardless of the environment, it is important to realize a paperlike white background. However, various reflective display devices, which have been examined and practically used up to now, have a chromophore mechanism fundamentally different from that of paper because they use a white pigment such as titanium dioxide (8, 9), thus a paperlike natural white color has not been obtained. In this study, we have done various examinations using newly developed organic/inorganic nanocomposites in order to develop an electronic paper with a natural white background similar to paper (see ref 10 for our preliminary results).

On the other hand, a reversible electrodeposition system including a bismuth compound and copper compound was used as an electrochromic material. The operating principle of the typical electrochromic device using this bismuth−copper system is based on the black indication caused by the codeposition of Bi−Cu in an acidic aqueous solution and the white indication caused by the dissolution of Bi−Cu (11−16). This device typically consists of $BiCl_3$, $CuCl_2$, LiBr, and HCl. Because it has a high coloration efficiency, rapid switching time, and long life cycle, it is expected to be a promising electrochromic device. In this study, we also paid attention to another bismuth compound and examined its possibility as an electrochromic material. The bismuth compound that we selected was bismuthyl perchlorate ($BiOClO_4$). This compound is readily soluble in water even in nonacidic aqueous solutions and is different from $BiCl_3$, which is soluble only in a strong acidic solution. Consequently, this is a material with few restrictions as an electrochromic material. This compound is utilized as a catalyst for the Michael addition reaction of indoles (17) and as a titrant for the quantitative assay of beryllium (18, 19). As a result of the study of these white background and electrochromic materials, a new electrochromic device with a high contrast ratio, rapid switching time, long open-circuit memory, long cycle life, low driving voltage, and a white background similar to paper was obtained. Its details (preparation and display properties of the display device) will be reported in this paper. This device is suitable for the display of document viewers, such as electronic books, because the background of the display medium is bright and the characters are easy to read.

2. EXPERIMENTAL SECTION

2.1. Structure of Display Device. The structure of the electronic paper prepared in this study is shown in Figure 1. It has a very simple structure, i.e., sandwiching a display medium between the image indicating side ITO (indium tin oxide) electrode (EHC Co., 10 Ω/sq) and a counter copper electrode,

* To whom correspondence should be addressed. E-mail: michiya-nakashima@ma.dic.co.jp (M. N.); k_hoshino@faculty.chiba-u.jp (K. H.).

Received for review February 5, 2010 and accepted April 12, 2010

† DIC Corporation.

‡ Chiba University.

DOI: 10.1021/am1001053

2010 American Chemical Society

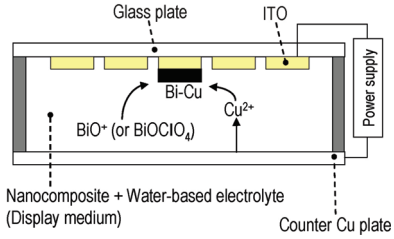

FIGURE 1. Display structure using polyamide/silica nanocomposite.

followed by sealing the surroundings. The display medium is a wet cake consisting of organic/inorganic nanocomposites and an aqueous electrolyte in which bismuthyl perchlorate is dissolved. These nanocomposites can be impregnated with more than nine times as much electrolyte on a weight basis. The features of the wet cake of the organic/inorganic nanocomposites include functioning as a white medium with a paper-like whiteness, an ionic conductor and a structure support material. The above-described bismuthyl perchlorate is electroreduced in an acidic aqueous solution and becomes the black metal bismuth (eq 1 (20) or eq 2 (21)). As for the previously reported electrochromic systems using bismuth species, studies have been exclusively devoted to the one that used the redox reaction of Bi^{3+} ions as indicated in eq 3 (11−16, 22). This time, we newly used bismuthyl perchlorate for the electrochromic material, and examined the possibility of its electrochromic reaction. In addition, copper ions coexisted in these systems (eq 1 or 2) in order to improve the repetitive characteristics as well as the system using Bi^{3+} (eq 3) (11−16). The reasons for using the copper sheet as the counter electrode are (1) to decrease the resistance of the counter electrode and decrease the resistance of the entire device, (2) to use an inexpensive metal material, (3) to contribute to the improvement in the repetitive characteristics by participating in the codeposition of Bi−Cu, using Cu^{2+}, which is eluted from the copper sheet during the eq 1 reaction on the ITO side.

$$BiOClO_4 + 2H^+ + 3e^- \leftrightarrow Bi + H_2O + ClO_4^- \quad (1)$$

$$BiO^+ + 2H^+ + 3e^- \leftrightarrow Bi + H_2O \quad (2)$$

$$Bi^{3+} + 3e^- \leftrightarrow Bi \text{ (or } BiClO_4^- + 3e^- \leftrightarrow Bi + 4Cl^-) \quad (3)$$

2.2. Synthesis of Display Medium Materials. Polyamide−silica organic/inorganic nanocomposite pulp, polyamide−silica organic/inorganic nanopowder, and polyamide pulp, which were used as the materials of the display medium, were synthesized by the following methods.

2.2.1. *Synthesis of Polyamide−Silica Organic/Inorganic Nanocomposite Pulp.* The organic/inorganic nanocomposite pulp was synthesized according to the report on the synthesis of the polyamide silica composites (23). The synthetic scheme of the composites is shown in Figure 2a. A 1.58 g sample of 1,6-diaminohexane (Wako Pure Chemical Industries) and 9.18 g of grade 3 sodium silicate (Nihon Chemical Industries) were added to 81.1 g of deionized water; this was stirred for 15 min at room temperature, and a homogeneous transparent aqueous solution was obtained. On the other hand, 2.49 g of adipoyl chloride (Wako Pure Chemical Industries) was added to 44.4 g of toluene (Kanto Chemical Co., >99.0%), then stirred for 5 min at room temperature, and a homogeneous transparent toluene solution was obtained. Next, the above-described aqueous solution was put in a blender bottle (Osterizer, 16 speed bender), and the toluene solution was dropwise added over 20 s while stirring at a rate of 10 000 rpm at room temperature. The polycondensation reaction of the polyamide was proceeded by this operation at the interface of the aqueous solution and the toluene solution, and a membranous gelatinous intermediate was formed. This intermediate was broken up using a spatula, and it was further stirred for 40 s at 10 000 rpm. The membranous intermediate was shredded by this operation, and a dispersed fluid in which a pulp-like product was dispersed was obtained. Water and toluene were removed from this dispersed fluid by filtering under reduced pressure through the filter paper with an aperture size of 4 μm, and a wet cake was obtained. This wet cake was dispersed into 100 g of methanol (Kanto Chemical Co., >99.5%), and washed by stirring for 30 min at room temperature, and then filtered under reduced pressure. Impurities and byproduct, such as toluene and NaCl, were removed by carrying out similar twice cleaning operations using 100 g of deionized water and additional once cleaning operation using extrapure water. Thus, 43.6 g of pure-white wet cake containing pulplike polyamide silica organic/inorganic nanocomposites, which includes extrapure water as a liquid component, was obtained. The material obtained by this method is called composite pulp A. The photograph of the obtained wet cake-like composites is shown in Figure 2b. The deionized water was prepared using Omron RT629-JO, and its electric conductivity was less than 1.5 μS/cm. The extrapure water was prepared using an extrapure water manufacturing apparatus (Nihon Millipore K.K., Milli-Q SP TOC), and its electric resistance was greater than 1.8 MΩ.

2.2.2. *Synthesis of Polyamide−Silica Organic/Inorganic Powdery Nanocomposites.* Powdery composites, which have a different shape, but the same composition with the pulp-like composites prepared in section 2.2.1, were prepared by changing the toluene in Figure 2a to acetone (Kanto Chemical Co., >99.0%). The same aqueous solution as that described in section 2.2.1, which included 1,6-diaminohexane and grade 3 sodium silicate, was prepared. Next, 2.49 g of adipoyl chloride was added to 44.4 g of acetone, the mixture was stirred for 5 min at room temperature, and a homogeneous transparent acetone solution was obtained. The above-described aqueous solution was added to a 300 cm^3 separable flask equipped with an anchor propeller, and the acetone solution was dropwise added over 20 s while stirring at 200 rpm. After the completion of this addition, the stirring operation was continued for ten minutes. In this operation, white powdery organic/inorganic nanocomposites were obtained during the process when the aqueous solution and the acetone solution were uniformly mixed. This composite was washed in the same way as described in section 2.2.1, and 27.1 g of a wet cake, which contained the powdery polyamide-silica organic/inorganic nanocomposites and extrapure water as the liquid component, was obtained. The material obtained by this method is called composite powder B.

2.2.3. *Synthesis of Polyamide Pulp.* Polyamide pulp, which had the same shape as the one described in section 2.2.1, but did not include silica, was synthesized. This material was synthesized using sodium hydroxide instead of sodium silicate in Figure 2a. By substituting sodium silicate by sodium hydroxide, the silica did not precipitate though the polymer synthesis reaction occurred. A 1.58 g sample of diaminohexane and 1.125 g of sodium hydroxide were added to 90 g of deionized water, the mixture was stirred for 15 min at room temperature, and a homogeneous transparent aqueous solution was obtained. Next, the same toluene solution in which adipoyl chloride was dissolved as described in section 2.2.1 was prepared. The above-described aqueous solution was added to the blender bottle at room temperature, and the toluene solution was dropwise added over 20 s while stirring at 10 000 rpm. A filmy

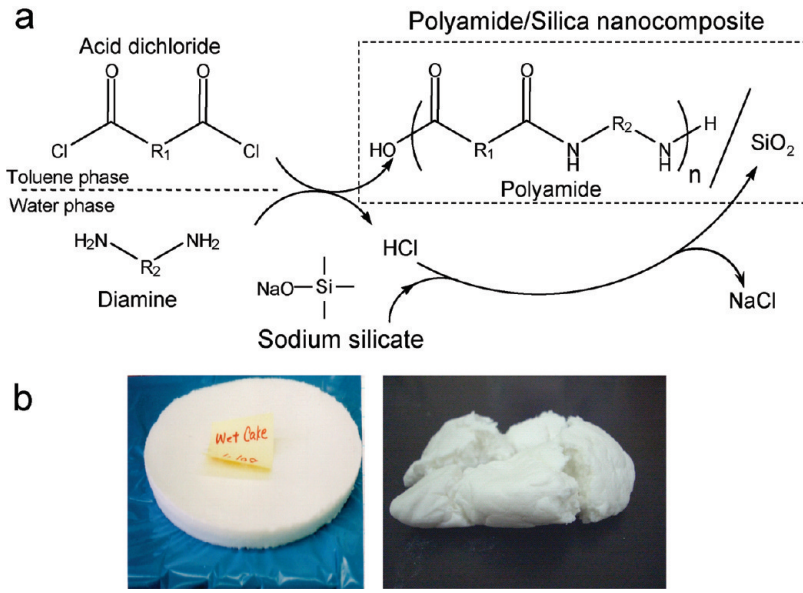

FIGURE 2. (a) Synthesis of the polyamide/silica nanocomposite and (b) the appearance of the resulting polyamide/silica nanocomposite wet cake.

Table 1. Characterization of Display Medium Materials A–C

nanocomposite	solid content (wt %)	silica content in nanocomposite[c] (wt %)	silica particle size (nm)
composite pulp A	10.3[a]	58	8
composite powder B	16.1[a]	62	12
polyamide pulp C	25.3[b]	0	

[a] Polyamide + silica. [b] Polyamide. [c] (Silica/(silica + polyamide)) × 100 (%).

gel-like intermediate similar to the one produced during the synthesis of composite A was obtained by this operation. This intermediate was broken-up using a spatula, and further stirred for another 40 s at 10 000 rpm. However, because it did not contain inorganic components, shearing was more difficult than composite pulp A. The stirring operation was then further continued for 60 s. As a result, a slurry containing the dispersed polyamide and having an appearance similar to the composite pulp A was obtained. This slurry was washed in the same way as in the case of the composite pulp A, and then 8.76 g of the wet cake containing the fibrous polyamide and extrapure water as the liquid component was obtained. The material obtained by this method is called polyamide pulp C.

2.2.4. *Measurement of Fraction of Solids in Display Medium Materials.* About 3 g of each wet cake of composite pulp A, composite powder B and polyamide pulp C was dried for five hours at 150 °C using a hot air dryer. The masses of the obtained dry materials, which did not contain water, were measured. The solids fraction of each material was calculated by dividing the mass (g) of the dry material by the mass (3 g) of the wet cake (Table 1). The solids fractions of the display media described in the next section were also measured in the same way.

2.3. Preparation of Display Devices and Devices for Measuring Ion-Transport Properties. 2.3.1. *Preparation of Electrolyte for Display Devices and Display Medium Material Dispersing Slurry.* A 0.33 g sample of bismuthyl perchlorate monohydrate (Mitsuwa Chemicals Co., >99.0%), which is an electrochromic material, 0.18 g of copper perchlorate (II) hexahydrate (Kanto Chemical Co., >99.0%), 0.34 g of the perchloric acid 60 wt % solution (Wako Pure Chemical Industries), 0.29 g of sodium perchlorate monohydrate (Wako Pure Chemical Industries, 98>%), 0.28 g of hydroquinone, and 0.009 g of 2-buthyne-1,4-diol (leveling agent) (24, 25) were added to 17 g of extrapure water. A homogeneous transparent electrolyte was prepared by stirring this mixture for 10 min at room temperature. Three kinds of display medium materials described in sections 2.2.1 to 2.2.3 were added to this electrolyte. The amount of the display medium material added at this time was adjusted to a solids content (dry mass) of 0.25 g. Because the amount of extrapure water added to the electrolyte with the display medium material at this time is different based on each display medium material, each sample was adjusted to have 20 g of the total quantity of extrapure water by adding more extrapure water. The slurry in which the solid content was uniformly dispersed was obtained by stirring for 30 min. The concentration of each compound in this electrolyte was 194 mM for the bismuthyl perchlorate, 96.7 mM for the copper perchlorate(II), 50 mM for the perchloric acid, 3000 mM for the sodium perchlorate, 130 mM for the hydroquinone, and 0.05 mM for the 2-buthyne-1,4-diol.

2.3.2. *Preparation of Display Media.* The display media were prepared in a glovebox (oxygen concentration: <1 vol %) with a flowing nitrogen gas atmosphere. A sheet of filter paper having an aperture size of 5 μm and a sheet of Teflon filter paper having an aperture size of 0.2 μm were stacked on the Kiriyama Rohto with a diameter of 60 mm. The entire quantity of the obtained display-medium dispersed slurry described in section 2.3.1 was put in the funnel, and the excess amount of electrolyte was separated by filtration under the reduced pressure of 0.02 MPa for 20 s, and then a nonwoven fabric-shaped sheet of about 350 μm thickness was obtained. A sheet-shaped wet cake (display medium) containing electrolyte was obtained by taking this sheet out of the funnel and folding it in the middle. Next, the display medium was weighed, and the solid content fraction in the display media was calculated (see section 2.2.4).

From the slurry containing the composite pulp A, the self-standing nonwoven fabric-shaped display medium having a homogeneous surface were obtained (hereinafter called "display medium A"). From the slurry containing the composite powder B, display medium B, which was fissile and had a poor self-standing property due to the powdery composites, was obtained. From the slurry containing the polyamide pulp C, the sheet-shaped display medium C, which had a poor electrolyte retention capability because the electrolyte was retained only

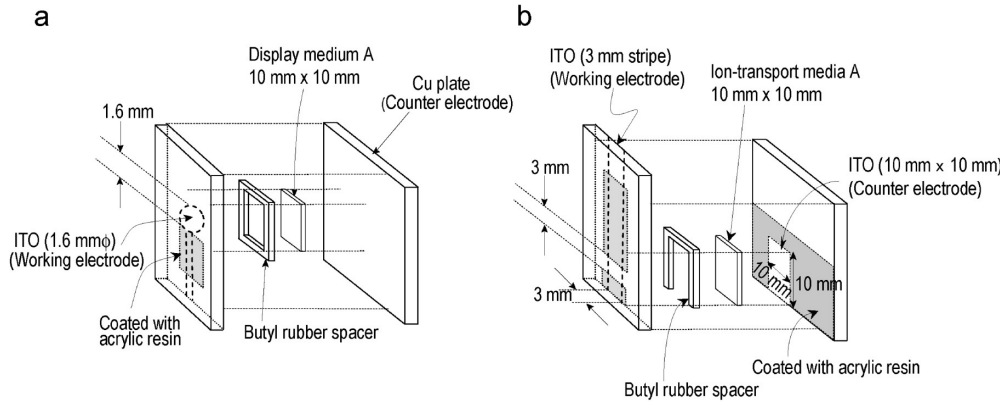

FIGURE 3. Cell structures for (a) the display device and (b) the device for measuring the ion-transport property.

in the voids of the nonwoven fabric pulp, was obtained. A self-standing and smooth sheet with a high electrolyte retention capability was obtained only from display medium A. Therefore, a display device was prepared only from the display medium A based on the method described in section 2.3.3. The light scattering property, which will be described in sections 2.5.1 and 2.5.2, was measured for all the obtained display media.

2.3.3. ***Preparation of Display Device (see Figure 3a).*** The display device was assembled in a glovebox (oxygen concentration <1 vol %) as well as the condition for the display media. The display medium with an area of 1 cm^2 was obtained by stamping out the display medium prepared from composite pulp A with a 1 cm ×1 cm die. The display electrode (working electrode) comprised a circular patterned ITO electrode of 1.6 mm in diameter (Figure 3a) and an ITO linear electrode to supply an electric current to the pattern. The linear electrode was coated with acrylic resin and insulated from the display medium. One drop of the electrolyte was added to the center of the above-described circular patterned ITO electrode and the display medium (1 cm ×1 cm) was then placed on it. At this time, it was done carefully so as not to create an air bubble between the display medium and the pattern electrode. Next, a butyl rubber spacer (Shinkaigomu Co., Ltd.) was placed on the periphery of the display medium, a copper sheet was placed on it, and the periphery of the display medium was sealed with a sealant (Seiwa Pro Co., Ltd.).

2.3.4. ***Preparation of Medium and Device for Evaluating Ion-Transport Property (see Figure 3b).*** To study the ion-transport property of composite pulp A, we prepared a device capable of measurement with the three-electrode system. An 8.85 mg sample of potassium ferrocyanide (Kanto Chemical Co., >99.5%) as the redox-active species and 1.743 g of potassium sulfate as the supporting electrolyte were dissolved in 17.82 g of extrapure water, and a uniform transparent aqueous solution was obtained. A 2.43 g sample of the composite pulp A was dispersed in it, and the slurry in which the composite pulp A was dispersed was obtained in a way similar to the display device preparation. The concentrations of potassium ferrocyanide and potassium sulfate in this slurry were 1 and 500 mM, respectively. This slurry was filtered under reduced pressure in a way similar to the display device preparation, and a wet-cake sheet (hereinafter called "ion-transport medium A") was obtained. The mass fractions of the polyamide and silica in this ion-transport medium A were calculated by measuring the total weight of the medium. This ion-transport medium A was stamped out with a 1 cm ×1 cm die. This piece was placed on the 3 mm ×3 mm size region of the ITO stripe working electrode having a 3 mm width where no acrylic resin coating had been applied. A butyl rubber spacer was placed on the periphery of the three sides of the ion-transport medium A, and an ITO counter electrode was then placed on it. The periphery of the ion-transport medium A was sealed with the sealant. The bottom side of the ion-transport medium was not sealed, and was open to the air. This was because the ion-transport medium A was placed in the KCl agar plate and electrically connected through its bottom side to the Ag/AgCl reference electrode as described below (Figure 9). The thickness of this ion-transport medium A was 680 μm.

2.3.5. ***Preparation of Device for Ion-Transport Property Comparison.*** A device, which had an aqueous solution containing 1 mM potassium ferrocyanide and 500 mM potassium sulfate instead of the ion-transport medium A in the cell shown in Figure 3b, was prepared as a comparative criterion of the device prepared in section 2.3.4 using the ion-transport medium A. The interelectrode distance was 680 μm. The bottom side of this cell was also not sealed. The KCl agar plate in Figure 9 was replaced by a beaker containing the electrolyte (1 mM $K_4[Fe(CN)_6]$ + 500 mM K_2SO_4), and the comparative criterion cell and salt bridge were soaked in the electrolyte to measure the ion-transport property.

2.3.6. ***Preparation of Titanium Dioxide White Gelatinous Sheet.*** As a comparison of the light scattering properties of the display media A, B, and C, a medium (8, 9) containing a titanium dioxide white pigment was prepared as follows: 90 g of extrapure water was heated to 70 °C, and 9.5 g of polyvinyl alcohol resin (Kuraray Co., Ltd., RS-2113UC) was added, which was dissolved by stirring. To a 9.8 g sample of the resin solution was added 0.2 g of minute titanium dioxide particles (Tayca Co., JR-301, rutile type, 0.3 μm in average diameter), and they were dispersed using a small homomixer. A viscous white resin solution in which the minute titanium dioxide particles were dispersed was obtained by this treatment. This solution was coated on the glass substrate using the applicator (gap: 200 μm), and a titanium dioxide containing gelatinous sheet with a smooth surface was obtained.

2.4. Evaluation of Display Media. 2.4.1. ***Measurement of Silica Content Rate.*** The dried display medium materials described in section 2.2.4 were weighed, put in an alumina crucible, and burnt in a muffle furnace for 3 h at 600 °C. Thus, the organic components were completely removed. After this treatment, the muffle furnace was cooled to 100 °C. Immediately thereafter, the mass of silica, which is the residue after ignition, was measured, and the silica content rate [(mass of silica/mass of dry material) × 100%] was calculated. As for both the composite pulp A and composite powder B, the shapes of the calcined products maintained those of the dry materials before calcining. However, the polyamide pulp C was completely burnt out by this heating.

2.4.2. ***Observation of Dispersion State of Silica Component and Measurement of Its Particle Size.*** Dry materials of the composite pulp A and composite powder B were pressed for 3 h at 170 °C and 20 MPa, and plate composites were obtained. These composites were cut into ultrathin sections of about 75 nm in thickness using the microtome. The obtained sections

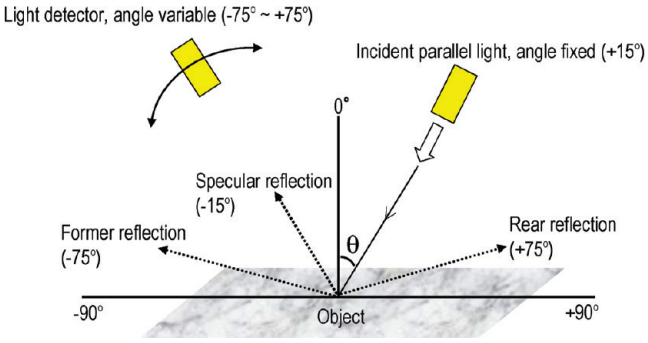

FIGURE 4. Measuring method of reflection brightness (*L*).

were observed using a transmission electron microscope (TEM). The silica component had a dark color, and the polyamide component had a light color. Fifty silica particles were selected in an arbitrary observation area, their particle sizes were measured, and the average value was considered to be the particle size of the silica.

2.4.3. *Shape Measurement of Display Medium Materials by Optical Microscopy.* The slurry of each material was obtained by adding 0.1 g of the composite pulp A, composite powder B, and polyamide pulp C to 5 g of deionized water, with stirring. Several drops of this slurry was dropped onto slide glasses using a dropper, and then covered with a cover glass. The shapes of the display medium materials were observed using a digital microscope.

2.5. Measurement of Optical Properties of Display Media. 2.5.1. *Measurement of Light Scattering Behavior of Display Media−1(26).* The light scattering properties of the display media A, B, and C described in section 2.3.2 and of the titanium dioxide containing gelatinous sheet described in section 2.3.6 were examined. The brightness of the display media from various angles was measured for parallel rays of light incident on the sample from a fixed direction (Figure 4). The measurement was done as follows using the gonio spectrophotometric color measurement system (model GCMS-11, Murakami Color Research Lab.). The vertical direction to the surface of the specimen was defined as $\theta = 0°$, the horizontal angle of incident light was defined as $\theta = 90°$, and the opposite direction was defined as $\theta = -90°$. The incidence angle of light on the specimen was set to $\theta = 15°$, and the brightness (L value) between $\theta = -75°$ and 75° was detected. Plain paper was selected as a typical paper medium, and its L value was similarly measured.

2.5.2. *Measurement of Light Scattering Property of Display Media−2 (27).* Another measuring method and analysis method by which the light-scattering property of the medium was able to be more clearly expressed were examined using the same measuring objects and measuring apparatus as those described in section 2.5.1. Each specimen was measured under the condition that the angle of incident light was changed from $\theta = 15°$ in section 2.5.1 to 75°, and the brightness (Y_S) of the reflected light was measured at various angles between $\theta = -75°$ and 75°. Next, the measured value was normalized by dividing the value by the measured value Y_0 of the standard white plate ($BaSO_4$), which was an instrument attachment, and the normalized value was expressed as r ($= Y_S/Y_0$) on the circular polar coordinates (radius r − light-receiving angle θ). Is this analysis, both the X- and Y-axes are dimensionless quantities because they express the normalized brightness value. When the measurement is done using the standard white plate, it becomes a half arc centered on the origin.

2.6. Measurement of Reflectivity and Contrast Ratio of Display Devices. 2.6.1. *Measurement of White Color Reflectivity of Display Devices.* The reflectivity of the display device A described in section 2.3.3 when the device was turned off (white color reflectivity) was measured using the display device evaluation system (Autronic-Melchers Co., DMS-500). The direction perpendicular to the display surface was defined as $\theta = 0°$, and the direction parallel to the display surface was defined as $\theta = 90°$. The reflection intensity of the display device A at $\theta = 0°$ was measured. The reflection intensity of the standard white plate ($BaSO_4$ plate, an instrument attachment) was measured in the same way. The white color reflectivity of the display device A was calculated using the following eq 4.

$$\text{white color reflectivity (\%)} = \text{(reflection intensity of display device A/ reflection intensity of standard white plate)} \times 100 \quad (4)$$

2.6.2. *Measurement of Black Color Reflectivity and Contrast Ratio for Black Display.* The electrochemical analyzer (BAS Co., model 760B) was connected to the display device A. A black color was formed on the working electrode by applying a voltage of −1.2 V versus the counter electrode for 500 ms. This black color was produced by the codeposition reaction of Bi, which was deposited based on eq 1 or 2, and Cu, which was deposited by the electroreduction of Cu^{2+}. This black color indication specimen was mounted on the display device evaluation system. The reflection intensity of the black material was measured by a method similar to that described in section 2.6.1, and the black color reflectivity was calculated. The contrast ratio was calculated based on the following eq 5 using the white color reflectivity and black color reflectivity of the display device.

$$\text{contrast ratio} = \text{white color reflectivity (\%)/black color reflectivity (\%)} \quad (5)$$

3. RESULTS

3.1. Characterization of Display Medium Material. The optical micrograph (a) and transmission electron microscope (TEM, JEOL JEM-200CX) images (b) of the composite pulp A are shown in Figure 5. It is understood from Figure 5a that the composite pulp A has a white pulplike shape with a high aspect ratio. It would appear that this pulplike shape was formed by stirring and shearing the filmy composites at high speed, which was formed at the interface between the toluene phase and the aqueous phase (see section 2.2.1). In Figure 5b, it was observed that the silica particles with an average particle diameter of about 10 nm, which were indicated by the dark area, were densely and uniformly dispersed throughout the composites and formed a three-dimensionally connected network structure. On the other hand, the composite powder B did not macroscopically form the pulplike shape, but formed a powdery shape that consisted of a spheroidal particle of several μm in diameter because it was synthesized in the medium in which the aqueous phase and the acetone phase were uniformly mixed (section 2.2.2).

However, the dispersion state of the silica particles determined from the TEM observation was almost similar to that of composite pulp A in Figure 5b. The polyamide C indicated a pulplike shape almost similar to Figure 5a because it was synthesized by the interfacial polymerization method similar to that of composite pulp A. The results based on these microscopic observations, and the results of

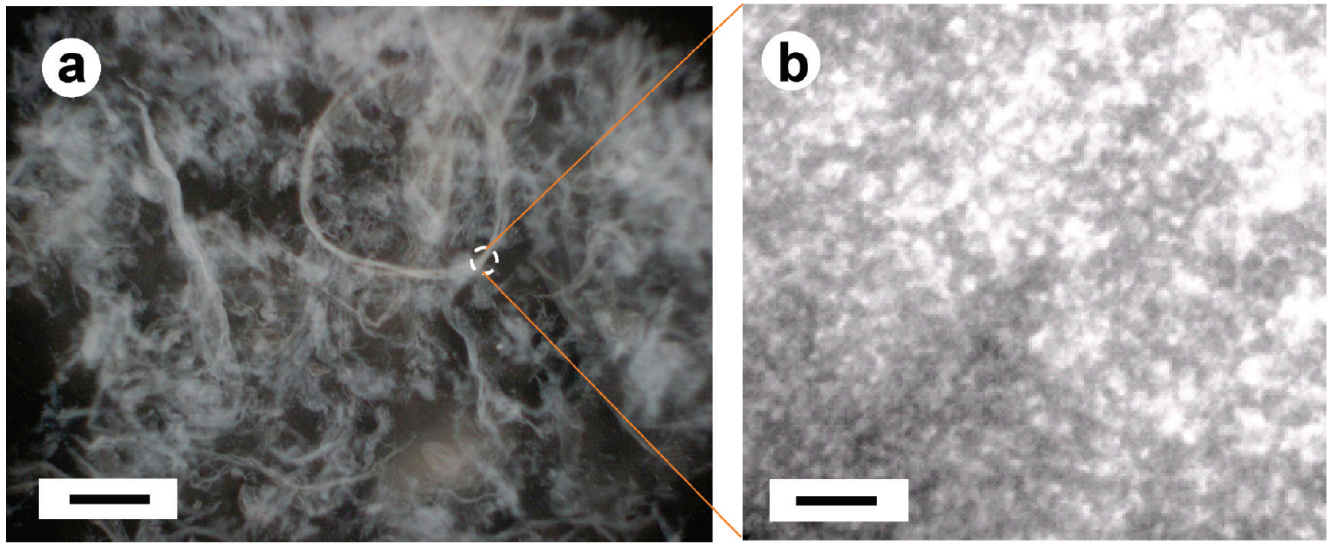

FIGURE 5. (a) Optical microscopic and (b) transmission electron micrographic (TEM) images of polyamide/silica nanocomposite (60 wt % SiO_2). Scale bars: (a) 100 μm, (b) 40 nm.

Table 2. Characterization of Display Media A−C

		physical property	
display medium	solid content (wt %)	self-sustainability	electrolyte-retention property
display medium A	10.8[a]	good	good
display medium B	16.7[a]	poor	good
display medium C	27.5[b]	good	poor

[a] Polyamide + silica + $BiOClO_4$ (194 mM) + $Cu(ClO_4)_2$ (96.7 mM) + $HClO_4$ (50 mM) + $NaClO_4$ (500 mM) + HQ (130 mM) + 2-buthyne-1,4-diol (0.05 mM). [b] Polyamide + $BiOClO_4$ (194 mM) + $Cu(ClO_4)_2$ (96.7 mM) + $HClO_4$ (50 mM) + $NaClO_4$ (500 mM) + HQ (130 mM) + 2-buthyne-1,4-diol (0.05 mM).

the measurements of the nanocomposites content rate (see section 2.2.4) and the silica content rate (see section 2.4.1) are shown in Table 1. It is understood that the composite pulp A and composite powder B have lower nanocomposite contents than that of the polyamide pulp C, that is, they have higher capabilities of retaining water, and that the silica component contributes to the water retention. Furthermore, it is understood that the composite pulp A has a higher water retention capability than that of the composite powder B, and that the pulplike shape is more advantageous for the retention of water than the powdery shape. Both the composite pulp A and the composite powder B have an extremely high silica content of about 60 wt % though their silica particles have an extremely small particle size of about 10 nm, therefore, these materials are difficult to prepare by the sol−gel method or melting-kneading method.

3.2. Characterization of Display Media and Ion-Transport Medium A. The solid content (nanocomposites + electrolyte), structural self-sustainability, and electrolyte-retention property of the display media A, B, and C are shown in Table 2. The solid contents of the display media A, B, and C were almost equal to the solid content of the composite pulp A, B, and polyamide C, respectively (Table 1), therefore it is understood that the retention property of water hardly depends on the presence of the electrolyte. It was found that the fraction of solids of the display media was also significantly dependent on the shape of the display medium material, and that the display medium A, which had the pulplike shape and the highest silica content, retained the highest amount of electrolyte. Additionally, it was found that the pulplike shape of the component material was necessary for maintaining the sheet shape, and that the nanosilica component was indispensable in order to retain the electrolyte as shown in Table 2. Consequently, it was clarified that the composite pulp A, which satisfied both requirements, was the most suitable material for the display medium. In addition, the solid content in the ion-transport medium A (polyamide + silica + $K_4[Fe(CN)_6]$(1 mM) + K_2SO_4(500 mM)) was 10.5 wt %, and the structural self-sustainability and electrolyte-retention property of the medium were good though not shown in Table 2.

3.3. Light Scattering Property of Display Media. The light scattering properties (detection angle dependency of brightness L, see section 2.5.1) of the display medium A (●) and display medium B (▲) are shown in Figure 6a. The light scattering property of the display medium C (■) and titanium dioxide dispersed white gelatinous sheet (Δ) are shown in Figure 6b. In addition, the light-scattering property of the plain paper (○) is shown in both a and b part for comparison. As for the display medium A in Figure 6a, the L value in the forward scattering ($\theta = -75°$) and back scattering ($\theta = 75°$) modes were high, and in particular, the value in the forward reflection was remarkably high. These light-scattering properties are similar to the properties of plain paper. Moreover, the display medium A indicated a higher L value than that of plain paper at all the detection angles. The display medium B also indicated light-scattering properties similar to plain paper; high values for both the forward reflection and the back reflection. However, they were lower values than that of plain paper at all the detection angles. Though plain paper becomes semitransparent without indicating light scattering in a wet condition, these display media retained their whiteness even when retaining the electrolyte. In particular, it is notable that the display

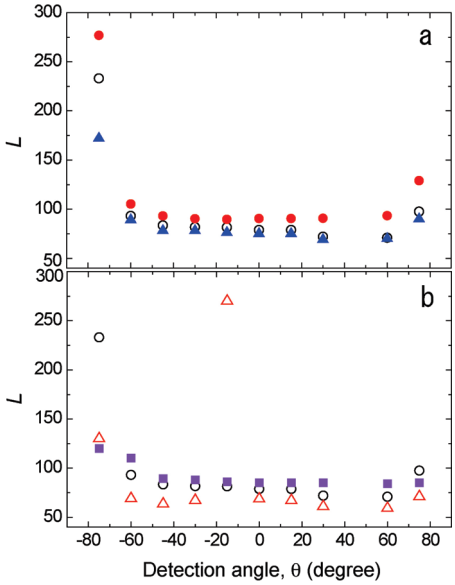

FIGURE 6. Dependence of L on detection angle, θ. (a) ○, Copy paper; ●, wet-cake sheet derived from the composite pulp A; ▲, wet-cake sheet derived from the composite powder B. (b) ■, Wet-cake sheet derived from polyamide C; Δ, TiO_2-dispersed PVA gel sheet. The error of L is ±1.

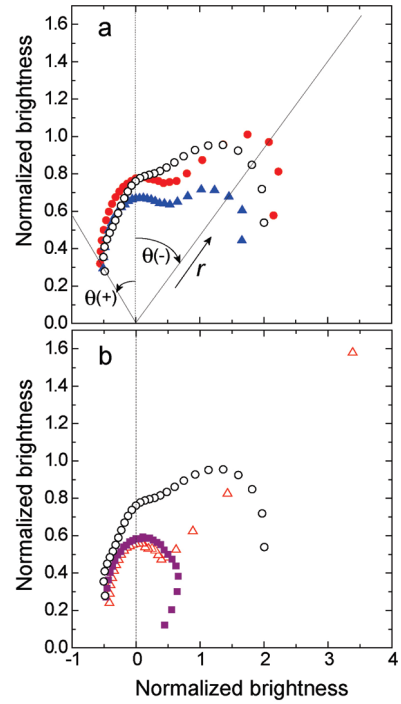

FIGURE 7. Normalized brightness plotted as a function of detection angle, θ (see section 2.5.2). (a) ○, Copy paper; ●, wet-cake sheet derived from the composite pulp A; ▲, wet-cake sheet derived from the composite powder B. (b) ■, Wet-cake sheet derived from polyamide C; Δ, TiO_2-dispersed PVA gel sheet. The error of r is ±0.05.

medium A indicated a higher light-scattering property even under the condition of retaining about a nine times higher amount of electrolyte as its own weight (see Table 2).

On the other hand, the titanium dioxide white gelatinous sheet and the display medium C indicated L values of about 1/2 of plain paper at $\theta = -75°$ and $+75°$ as shown in Figure 6b, and the light scattering properties were not similar to those of plain paper. As for the display medium C, the light-scattering properties similar to plain paper were not obtained though it had a lower electrolyte content than that of the display media A and B. Furthermore, for the titanium dioxide white gelatinous sheet, the L value at $-15°$, which corresponded to the specular reflection of the incident light, was remarkably high, and the light scattering property was essentially different from that of plain paper.

The analysis results of the display media A (●) and B (▲), which were derived from the brightness function calculated according to the method described in section 2.5.2, are shown in Figure 7a. In addition, the results of the analysis on the titanium dioxide white gelatinous sheet (Δ) and the display medium C (■)are shown in Figure 7b. The analysis result on the plain paper (○) is also indicated in both a and b parts for comparison. In these figures, the distance from the origin indicates the intensity of the scattered light, and the plus region of the X-axis indicates a forward light scattering. The plain paper result indicated that the forward light scattering was remarkably strong, and it was determined that the medium material, which indicated a light scattering property similar to this, had a paperlike texture. As for the display media A (●) and B (▲), it is understood that the curve has a bulge in the plus region of the X-axis, and that their fundamental light scattering properties are similar to that of plain paper. In particular, it is understood that the display medium A indicated a higher forward scattering intensity than that of plain paper, and that it had a more paperlike light scattering property than that of plain paper. The display medium B had a lower forward scattering intensity than that of the display medium A and plain paper, and therefore, it was inferior in the paperlike texture. The value of the X-axis ranging from 0.2 to 1.5 corresponds to the detection angle close to perpendicular to the paper plane. In this region, the highest scattering intensity was observed for the plain paper.

On the other hand, the display medium C (■) and titanium dioxide white gelatinous sheet (Δ) indicated a light-scattering behavior that was quite different from that of the plain paper. The forward scattering intensity of the titanium dioxide white gelatinous sheet drastically increased in the region of 0.5 or more on the X-axis, though it was generally low. This increase in the forward scattering indicates the specular reflection of the incident light caused by the smooth surface of the sheet. Consequently, it is understood that the titanium dioxide white gelatinous sheet has a surface on which only the specular reflection is intense, and that it indicates a scattering behavior significantly different from that of paper. For the display medium C, the bulge of the characteristic curve of the forward scattering, which was observed for the display media A and B, was hardly observed, and no paper-like light scattering property was indicated. In Figure 8, photographs of the display medium A (left) and plain paper (right) with a size of 10 cm ×10 cm are shown. The display medium A and the plain paper cannot be distinguished by visual comparison, and it is demonstrated that the display medium A has the same texture as paper.

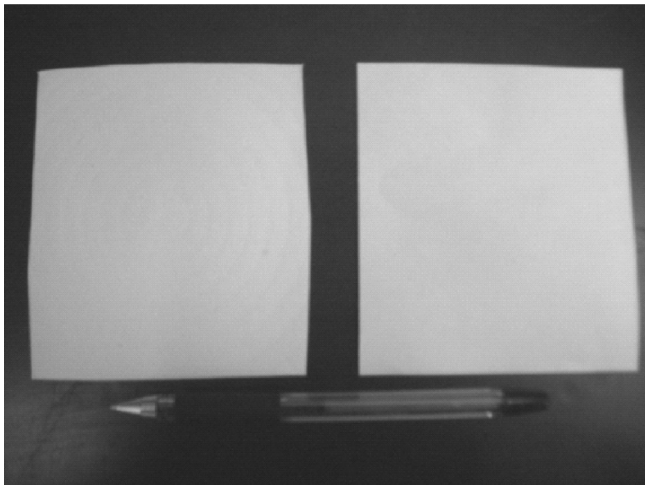

FIGURE 8. Comparison of the appearance between our nanocomposite display medium (left) and a copy paper (right).

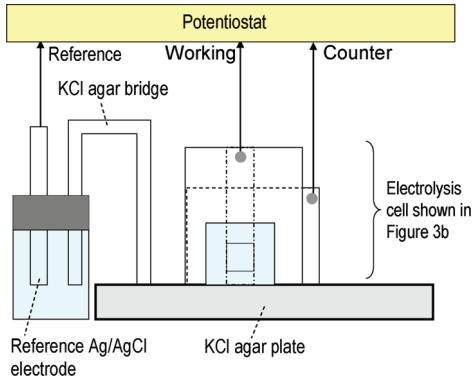

FIGURE 9. System for measuring the ion-transport property of the ion-transport medium A containing 1 mM ferrocyanide and 0.5 M K_2SO_4.

3.4. Characteristics of Composite Pulp A as Ion-Transport Medium. The ion-transport property of the composite pulp A was evaluated by cyclic voltammetry using the ion-transport measuring device described in section 2.3.4. The ion-transport measuring device shown in Figure 3b was connected to a gelatin plate containing KCl through its base (portion without the butyl rubber spacer). The gelatin plate was connected to the Ag/AgCl reference electrode through the gelatin salt bridge containing KCl (Figure 9). The cyclic voltammetry measurements were done at various sweep rates (v; $v = 1$, 10, 100, 1000, and 10000 mV/s). Moreover, for comparison, the cyclic voltammetry was done for a device that contained only the electrolyte and did not include the composite pulp A, though it had the same construction as that of the ion-transport medium measuring device (see section 2.3.5). The relation between the sweep rates (v) and the difference in the peak potential (ΔE_p) between the oxidation peak current and reduction peak current of the potassium ferrocyanide was examined, and the ion-transport property of the composite pulp A was evaluated (28, 29).

The cyclic voltammogram of the redox pair $[Fe(CN)_6]^{3-/4-}$ measured in the ion-transport medium A is shown in Figure 10a. For comparison, the cyclic voltammogram of the potassium ferrocyanide aqueous solution, which did not contain the composite pulp A, is shown in Figure 10b. Both cyclic voltammograms a and b in Figure 10 indicated almost the same oxidation−reduction peak current values and peak potentials for the same sweep rate. Also, the waveforms of the cyclic voltammogram at each sweep rate were also almost similar. The relation between the sweep rate (v) and the difference in the peak potential (ΔE_p) between the oxidation and reduction peak current is shown in Figure 10c. The ΔE_p values are larger than that for the reversible case, 0.06 V, and increase with v, indicating that the electrode reaction for the $[Fe(CN)_6]^{4-/3-}$ redox couple is quasi-reversible. This nonreversible nature may be due to the sluggish electron transfer kinetics at the ITO/electrolyte interface, not due to the conductive property of the electrolyte solution (30). The ΔE_p indicated a similar sweep rate dependency for the ion-transport medium A (○) and the electrolyte (●). Moreover, the difference in ΔE_p between both liquids was low, and was hardly observed in the area where the sweep rate was low. Though the difference between them slightly increased as the sweep rate increased, the difference was only 0.019 V even at the rate of 10 000 mV/s. On the basis of the above-described results, it was indicated that the composite pulp A hardly affected the solution resistance, and that it was a good-quality ion-transport medium. In addition, these results also implies that the ion transport medium A may be a highly resistive material for electron conduction and satisfy the essential requirement for an electrochemical device.

3.5. Evaluation Results of Display Devices. ***3.5.1. Cyclic Voltammetry of Display Device A.*** The cyclic voltammogram of the display device A is shown in Figure 11a. This voltammogram was measured using the two-electrode cell method (Figure 3a) without the reference electrode. The voltage on the X-axis is the potential based on the counter copper electrode. When the potential of the circular working electrode was swept from 0 V to the direction of the cathode potential, a big reduction current was observed at −0.8 V (peak potential value of the electrolysis current). Next, the potential was reversed at −1.0 V, and was swept in the anodic direction. A high oxidation current at +0.6 V and a low oxidation current at 0.8−1.2 V were observed. Ziegler reported the cyclic voltammetry of the aqueous solution containing 10 mM $BiCl_3$, 10 mM $CuCl_2$, and 0.5 M HCl using ITO as the working electrode and the Ag/AgCl reference electrode (14). The voltammogram obtained at that time indicated a waveform similar to the one in Figure 11a though the potential value of the X-axis and range was different because the electrode, to which the potential was referenced, was different. It is presumed from Ziegler's voltammogram that the reduction current observed at −0.8 V corresponded to the codeposition reaction of Bi and Cu as shown in eq 1 or 2, and that the oxidation current at +0.6 V corresponded to the reverse reaction. Though the black deposit of Bi−Cu was almost dissolved by oxidizing at +0.6 V, it was not completely dissolved. Its dissolution was completed after the oxidation current at +0.8−1.2 V. Figure 11b shows the cyclic voltammogram of a display device (display device B), which was prepared by excluding

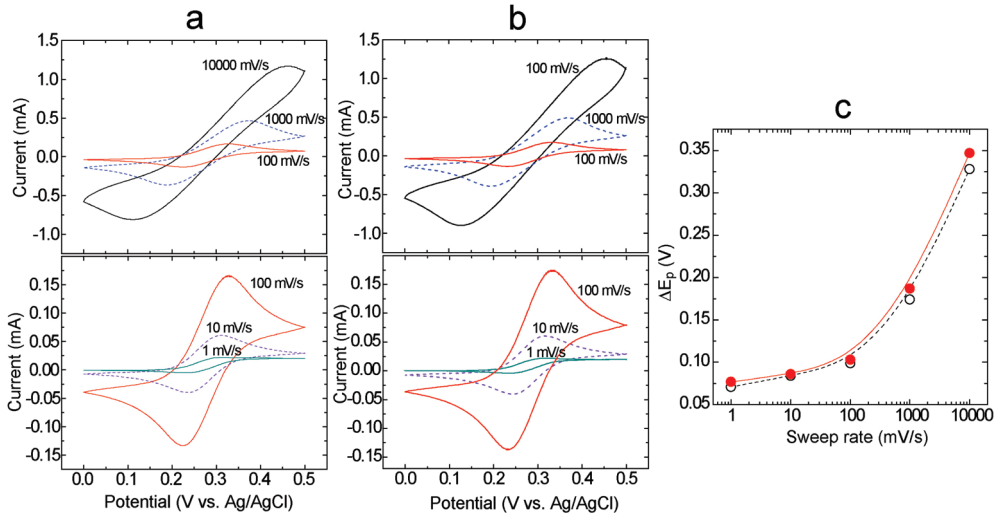

FIGURE 10. Cyclic voltammograms of ferrocyanide (1 mM) in (a) the ion-transport medium A containing 0.5 M K_2SO_4 and in (b) the aqueous solution containing 0.5 M K_2SO_4 measured at various sweep rates. The numerical values in the figures indicate the sweep rate. Electrode area: 0.09 cm^2. (c) Relationship between the peak separation, ΔE_p, and sweep rate for the $[Fe(CN)_6]^{3-/4-}$ couple in the ion-transport medium A (open circle) and in the aqueous solution (closed circle) containing 0.5 M K_2SO_4. The error of ΔE_p is ±0.005 V.

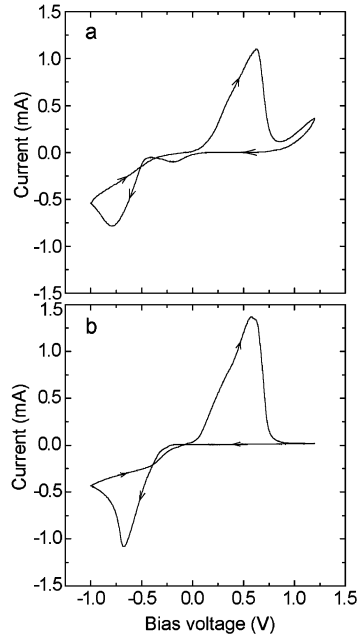

FIGURE 11. Cyclic voltammograms of (a) a display medium A and (b) a display medium prepared by removing HQ from the display medium A at an ITO electrode (area: 0.02 cm^2). Sweep rate: 100 mV s^{-1}. Counter electrode: Cu plate.

hydroquinone (HQ) from the electrolyte of the display device A. It was different from the voltammogram in Figure 11a, that is, the oxidation wave at 0.8−1.2 V and the reduction wave at 0 to −0.3 V were not observed. The black deposit of Bi−Cu accumulated without completely dissolving, and a residue (ghost image) appeared after about 10 cycles of the potential sweep. Based on these results, it is understood that the oxidation wave observed at +0.8−1.2 V corresponded to the oxidation of HQ to benzoquinone (BQ), and that the produced BQ contributed to complete dissolution (or oxidation) of the Bi−Cu deposit by chemical oxidation. It is also understood that the reduction wave at 0 to −0.3 V corresponded to the electroreduction of a fraction of BQ, which did not take part in the oxidative dissolution of Bi−Cu in the produced BQ. When the counter copper electrode was changed to the ITO electrode and a similar examination was done, a reduction current peak of the codeposition reaction of Bi and Cu (coloration reaction) at −1.1 V and an oxidation current peak of the dissolving reaction of Bi−Cu (decoloration reaction) at +1.3 V were observed. The reduction potential and the oxidation potential, respectively, shifted to the cathodic side and the anodic side when compared with the above-described display device A. This is attributed to the fact that the resistivity of the ITO counter electrode was higher than that of the copper electrode. A reductive reaction of the ITO occurred due to an increase in the driving voltage (±1.35 V), and light coloration of the ITO was observed. Moreover, after the potential sweeping cycle exceeded 1×10^4 times, dendric deposits of Bi−Cu were formed, and the coloration and decoloration did not work because of the short-circuit of the two ITO electrodes. HQ was excluded from the above-described devices of ITO/display medium A/ITO, and repetitive cyclic voltammetry was done. Every time the potential sweep was repeated, the rate of the decoloration reaction decreased, and after the frequency of the potential sweep exceeded about 1×10^2 times, the residue after erasing appeared. These results also indicate that HQ had the function of a mediator of the Bi−Cu dissolving reaction.

3.5.2. Various Characteristics of Display Medium A. The white reflectivity, black reflectivity, and contrast ratio of display device A measured by the methods described in sections 2.6.1 and 2.6.2 are shown in Table 3. A high white indicating reflectivity (65%) and a low black indicating reflectivity (6.4%) were obtained, and a high contrast ratio of 10:1 was achieved. Moreover, the voltage required for indicating this high contrast ratio was as low as 1.2 V and the voltage application time of 500 ms was comparatively short time. When a rectangular wave voltage of ±1.2 V, 0.83 Hz was applied, its operating life was more than 1×10^6 cycles. Furthermore, the retention time of the

Table 3. Performance of the Display Device Based on the Nanocomposite Pulp A

white state reflectivity (%)	65
black state reflectivity (%)	6.4
contrast	10:1
driving voltage (V)	1.2
response time (ms)	500
open-circuit memory (day)	30
operating life (cycle)	$\sim 1 \times 10^6$

open-circuit memory was at least 30 days or more. In the bismuth electrochromic display device, copper ion is added in order to prevent the ghost image as described in section 3.5.1. However, the addition of copper ions caused the open-circuit self-erasure, and the memory characteristics did not appear. However, an extremely long recording lifetime was obtained for the display device A. However, the reason for this is not yet understood, and it is a problem to be examined in the future.

A black indicating circle image formed on the display device A is shown in Figure 12. Though some spotted images due to the ruggedness of the composite pulp nonwoven fabric were observed on the picture part, its level was low enough to be visually ignored. Such spotted images are usually observed for printed matter from an ink jet printer. In general, though it is one of the shortcomings that a metallic luster appears on a metal-deposition type electrochromic device with a black coloring, this display device indicated a low metallic luster due to this spotted image. Figure 13 shows photographs of the off-state (a) and on-state (b) of the display device prepared using a fixed pattern electrode. The screen size is six inches. A soft whiteness could be realized in the off-state by the light scattering similar to paper. Moreover, a high-definition image having a high contrast ratio and good visibility was obtained in the on-state.

4. DISCUSSION

The display medium formed using inorganic/organic nanocomposites combined three functions: a white medium with a paper-like texture, an ion-transport medium, and a separator (insulator against electronic conduction + structure support material). We presumed that these characteristics were derived from the following features of the inorganic/organic nanocomposites, and believe that its substitution with other materials is difficult. In the following sections, the formation mechanisms of these three functions were considered.

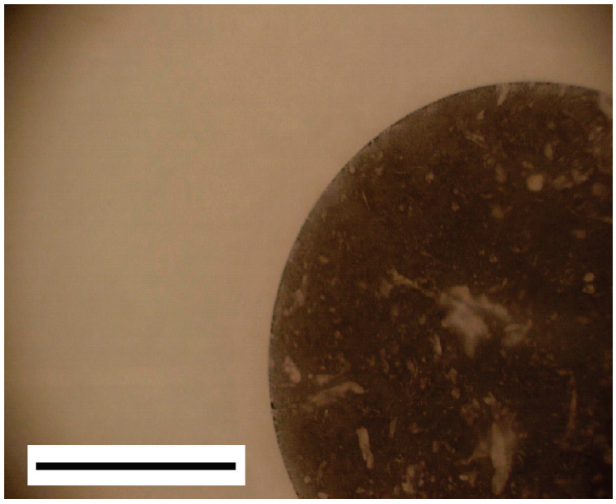

FIGURE 12. Magnified view of the flakes in the image region of the display device based on the nanocomposite pulp A. Scale bar: 0.5 mm.

4.1. Function of White Medium with Paperlike Texture. On the basis of the result described in section 3.3, it has been determined that display medium A had a forward scattering behavior, which was specific to the paperlike texture and exceeded that of plain paper, even when containing a high amount of electrolyte, and that the requirement for this behavior was: (1) nanosized silica microparticles had to exist in the medium, and (2) the forward scattering had to be promoted by the effect of the pulp shape of the composites.

(1) Effect of Nanosized Silica Microparticles. In the inorganic/organic nanocomposites, the silica microparticles of 10 nm or less did not exist as a single particle, but they were connected to each other, and a continuous interface of the organic/inorganic composites was formed throughout the display medium (Figure 5). Therefore, it is believed to have a strong light scattering property, even though the silica with a particle size of less than 10 nm should be optically transparent, the refractive index difference between silica (refractive index: about 1.45) and polyamide (refractive index: 1.53) was low, and it retained a high amount of ion component and water as the electrolyte solvent.

(2) Effect of Pulp Shape. There were innumerable voids randomly dispersed on the surface and inside of the display medium. It is thought that a strong light scattering was promoted because reflection in an unspecified direction occurs at the boundary of the electrolyte and the nanocomposites in these voids. This indicates that the same light scattering phenomenon, which occurred in ordinary paper due to its pulp shape, similarly occurred in the nanocomposite pulp. However, it is thought that the effect of the silica indicated in (*1*) was greater than that of the pulp, because display medium C did not indicate a paper-like light scattering, though it contained the polyamide pulp.

4.2. Function of Ion-Transport Medium. Though the plain electrolyte is the best ion-transport medium, it has a risk of liquid leakage. Therefore, it is technologically inappropriate to use it without modification. Therefore, it is an important matter how to retain a large amount of electrolyte without affecting the ion transport property of the medium. In these materials, silica, which has a strong affinity for the polar solvent, was contained at the high content of about 60 wt %. Moreover, a high silica surface area existed and a large amount of water could be adsorbed because these silica particles had an extremely minute particle size of about 10 nm. Consequently, it is understood that these materials could retain a large amount of electrolyte even though it contained a high concentration of salt unlike water-absorbing resins. It is also thought that because this retaining

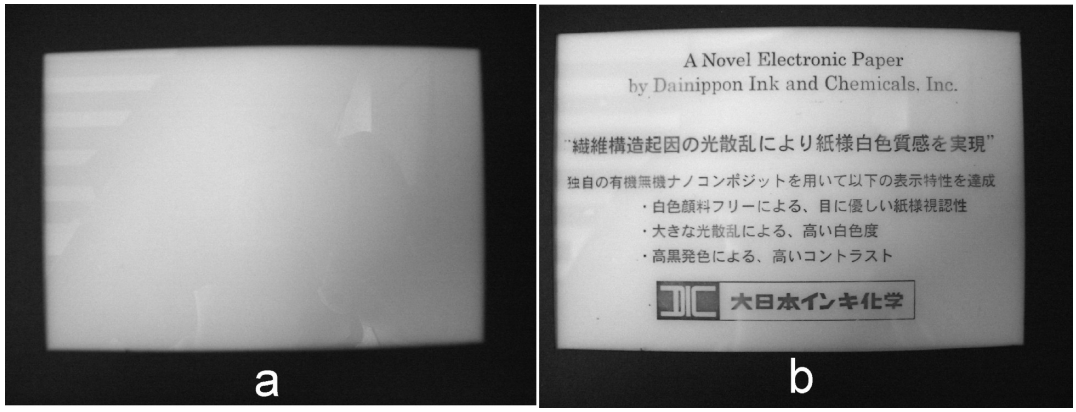

FIGURE 13. Visual aspect of the electrochromic device (6 in. diagonal size) based on the nanocomposite pulp A. Bias voltage: (a) 0, (b) 1.2 V.

function was caused only by the physical water adsorption and not by a strong bonding, such as a chemical bond or coordinate bond, and that the ion-transport property of the electrolyte was not reduced. The reason why composite pulp A had a superior electrolyte retention capacity than the composite powder B is attributable to the peculiar shape between the fibers due to the pulp shape. It is presumed that composite pulp A could retain the electrolyte nine times or more its own weight by the effect of its peculiar shape, and that its high ion-transport property almost equaled that of the plain electrolyte.

4.3. Function of Separator (Insulator Against Electronic Conduction + Structure Support Material). The display medium A, which was prepared by retaining the electrolyte in the composite pulp A, served as a separator in addition to the function described in sections 4.1 and 4.2. The separator is required to function as a highly resistive material for electron conduction and a structure support material. The main component of the solid material in the composite pulp A is silica microparticles with a low alkali metal content. The volume resistivity of silica is 1×10^{18} Ω cm (31). It is very high compared to the resistivities of soda glass and borosilicate glass (1×10^{13} to 1×10^{14} Ω cm (31)) and conventional resin materials (1×10^{12} to 1×10^{16} Ω cm (31)). Therefore, it is suitable for use as a highly resistive material for electron conduction, and a high stability can be expected as a device with a high brekdown strength.

Furthermore, the composite pulp A is a nonwoven fabric with a high tensile strength due to its pulp shape, even when retaining electrolyte. Therefore, it works as a structure support material in order to accurately limit the interelectrode distance, and a support medium between the electrodes like spacers is unnecessary.

5. CONCLUSION

The display medium materials A, B, and C were prepared, and their compositions, shapes, and ability to retain water were examined (section 3.1). As a result, it was understood that the display medium materials A and B were nanocomposites of silica and polyamide. The silica content was about 60 wt %. The display medium materials A and C had a pulp shape. It was understood that the ability to retain water depended on the presence of silica and the shape of the material, and that the display medium material A, which had the pulp shape, had the highest water retention capability.

The display media A, B, and C were prepared from the display medium materials A, B, and C, respectively (section 3.2). It was understood that display medium A with silica and the pulp shape had the highest electrolyte retention capability, as well as the result presented in section 3.1. It was also understood that the pulp shape was necessary for retaining the sheet shape, and that the display medium A was still the most appropriate. In addition, in this study, the bismuthyl perchlorate was selected as a bismuth compound, which was impregnated in the display media as an electrochromic material, instead of the conventionally used bismuth(III) chloride.

The light-scattering properties of the display media A–C, paper, and the titanium dioxide white gelatinous sheet were measured (section 3.3). As a result, the following characteristics have been clarified.

(1) The paperlike texture as typified by the plain paper appeared due to the high forward scattering of the reflected light.

(2) Because the display media obtained from the inorganic/organic nanocomposites had a light scattering property similar to that of paper, they had a visibility close to that of paper. In particular, display medium A with the pulp shape had a higher forward scattering than that of the plain paper.

(3) On the basis of the comparison of the light-scattering properties of display media A–C, the occurrence of the forward scattering, which was the main part of the paperlike light scattering, was affected by the shape of the polyamide (pulp shape or powdery shape) and the presence of the silica nanoparticles, and that of the latter had a greater effect.

(4) Because the titanium dioxide white gelatinous sheet had a strong specular reflection, which was never observed on paper, and did not have the forward scattering specific to paper, it was unsuitable as the background of electronic paper.

The cyclic voltammetry of the ferrocyanide ion was carried out for the composite pulp A and aqueous solution, and their electrode reaction behaviors were compared and examined (section 3.4). As a result, it was understood that

almost no difference was observed in the electrode reaction behavior of both materials, and that the composite pulp A was an excellent ion-transport medium.

The image display test as an electrochromic type electronic paper was done using the display medium material A (section 3.5). As a result, it was revealed that the above-described display device indicated a light-scattering property similar to paper, and that an excellent electronic paper with a white color reflectivity of 64%, a contrast ratio of 10:1, an operating life of more than 1×10^6 cycles, and an open-circuit memory of at least greater than one month could be obtained. In addition, the writing time was 500 ms, and the driving voltage was 1.2 V.

REFERENCES AND NOTES

(1) Comiskey, B.; Albert, J. D.; Yoshizawa, H.; Jacobson, J. *Nature* **1988**, *394*, 253.
(2) Cummins, D.; Boschloo, G.; Ryan, M.; Corr, D.; Rao, S. N.; Fitzmaurice, D. *J. Phys. Chem. B* **2000**, *104*, 11449.
(3) Grätzel, M. *Nature* **2001**, *409*, 575.
(4) Jo, G.-R.; Hoshino, K.; Kitamura, T. *Chem. Mater.* **2002**, *14*, 664.
(5) Ito, M.; Miyazaki, C.; Ishizaki, M.; Kon, M.; Ikeda, N.; Okubo, T.; Matsubara, R.; Hatta, K.; Ugajin, Y.; Sekine, N. *J. Non-Cryst. Solids* **2008**, *354*, 2777.
(6) Lee, D.-S.; Shieh, K.-K.; Jeng, S.-C.; Shen, I.-H. *Displays* **2008**, *29*, 10.
(7) Sun, X. W.; Wang, J. X. *Nano Lett.* **2008**, *8*, 1884.
(8) Jacobson, J. M.; Cominskey, B. U.S. patent 5 930 026, 1999.
(9) Sheridon, N. K.; Berkovitz, M. A. *SID '77 Digest*; Society for Information Display: Campbell, CA, 1977; p 114.
(10) Nakashima, M.; Saito, N.; Kawai, K.; Ebine, T.; Suzuki, Y. Novel electronic paper using organic/inorganic nanocomposite. *Report from the Anual Conference of the Imaging Society of Japan*; Tokyo, June 2−4, 2004; Imaging Society of Japan: Tokyo, 2004; pp 205−208.
(11) Howard, B. M.; Ziegler, J. P. *Sol. Energy Mater. Sol. Cells* **1995**, *39*, 309.
(12) Ziegler, J. P.; Howard, B. M. *Sol. Energy Mater. Sol. Cells* **1995**, *39*, 317.
(13) Córdoba de Torresi, S. I.; Carlos, I. A. *J. Electroanal. Chem.* **1996**, *414*, 11.
(14) Ziegler, J. P. *Sol. Energy Mater. Sol. Cells* **1999**, *56*, 477.
(15) de Oliveira, S. C.; de Morais, L. C.; da Silva Curvelo, A. A.; Torresi, R. M. *J. Electrochem. Soc.* **2003**, *150*, E578–E582.
(16) de Oliveira, S. C.; de Morais, L. C.; da Silva Curvelo, A. A.; Torresi, R. M. *Sol. Energy Mater. Sol. Cells* **2005**, *85*, 489.
(17) Mohammadpoor-Baltork, I.; Memarian, H. R.; Khosropour, A. R.; Nikoofar, K. *Heterocycles* **2006**, *68*, 1837.
(18) Sankar Das, M.; Athavale, V. T. *Anal. Chim. Acta* **1955**, *12*, 6.
(19) EL-Yamani, I. S.; ABD EL-Messieh, E. N. *Talanta* **1978**, *25*, 704.
(20) Poznyak, S. K.; Kulak, A. I. *Electrochim. Acta* **1990**, *35*, 1941.
(21) Romann, T.; Väärtnõu, M.; Jänes, A.; Lust, E. *Electrochim. Acta* **2008**, *53*, 8166.
(22) Jang, S.; Huang, Y.-H.; Luo, F.; Du, N.; Yan, C.-H. *Inorg. Chem. Commun.* **2003**, *6*, 781.
(23) Idemura, S.; Haraguchi, K. U.S. patent 6 063 862, 2000.
(24) Kruglikov, S. S.; Kudriavtsev, N. T.; Vorobiova, G. F.; Antonov, A. Ya. *Electrochim. Acta* **1965**, *10*, 253.
(25) Atanassov, N.; Bozhkov, Hr.; Vitkova, St.; Rashkov, St. *Surf. Tech.* **1982**, *17*, 291.
(26) Nicodemus, F. E.; Richmond, J. C.; Hsia, J. J.; Ginsberg, I. W.; Limperis, T. *Geometric Considerations and Nomenclature for Reflectance*; NBS Monograph 160National Bureau of Standards:: Washington, D.C., 1977.
(27) Lafortune, E.; Foo, S.-C.; Torrance, K.; Greenberg, D. Non-Linear Approximation of Reflectance Functions. In *Report from SIGGRAPH97*; Los Angeles, Aug 3−8, 1997; Association for Computing Machinery's Special Interest Group on Graphics and Interactive Techniques: New York, 1997; p 117.
(28) Nicholson, R. S. *Anal. Chem.* **1965**, *37*, 1965.
(29) Bard, A. J.; Faulkner, L. R. *Electrochemical Method*; John Wiley & Sons: New York, 1980; p 230.
(30) Zudans, I.; Paddock, J. R.; Kuramitz, H.; Maghasi, A. T.; Wansapura, C. M.; Conklin, S. D.; Kaval, N.; Shtoyko, T.; Monk, D. J.; Bryan, S. A.; Hubler, T. L.; Richardson, J. N.; Seliskar, C. J.; Heineman, W. R. *J. Electroanal. Chem.* **2004**, *565*, 311.
(31) http://www4.ocn.ne.jp/~katonet/index.html.

AM1001053